Positive Zero-field Splitting and Unexpected Slow Magnetic Relaxation in the Magneto-chemical Calibrant $HgCo(NCS)_4$

Journal:	*Dalton Transactions*
Manuscript ID	DT-COM-02-2021-000407.R1
Article Type:	Communication
Date Submitted by the Author:	20-Feb-2021
Complete List of Authors:	Boca, Roman; University of SS Cyril and Methodius, Department of Chemistry Titis, Jan; University of SS Cyril and Methodius, Trnava, Department of Chemistry Rajnák, Cyril; University of SS Cyril and Methodius, Department of Chemistry Krzystek, Jurek; National High Magnetic Field Laboratory, Condensed Matter Science

COMMUNICATION

Positive Zero-field Splitting and Unexpected Slow Magnetic Relaxation in the Magneto-chemical Calibrant HgCo(NCS)$_4$

Received 00th January 20xx,
Accepted 00th January 20xx

DOI: 10.1039/x0xx00000x

Roman Boča,*[a] Ján Titiš,[a] Cyril Rajnák,[a] and J. Krzystek[b]

DC magnetization data for HgCo(NCS)$_4$ confirm positive value of the zero-field splitting *D*-parameter. High-frequency and -field EPR gave g_z = 2.05, g_x = 2.16 and D/hc = 5.39 cm^{-1}. The complex exhibits a field-induced slow magnetic relaxation with two relaxation modes and unusual temperature evolution of the relaxation time.

The calibration of magnetochemical hardware is traditionally based upon the mercury(II)-tetrakis(iso-thiocyanato) cobaltate, HgCo(NCS)$_4$. Several basic papers have been devoted to this issue.[1-7] The most recent publication utilized the powder susceptibility data, along with the single-crystal data taken by a SQUID magnetometer, in order to retrieve the set of magnetic parameters, such as the axial zero-field splitting parameter *D*, the magnetogyric factor g_{iso}, (g_z and g_x for a single crystal) and eventually the molecular-field correction *zj*.[7] However, there is a number of objections against the assessment that this study is already complete as follows.

(i) The axial zero-field splitting parameter *D* occurring as a part of the spin Hamiltonian $\hat{H} = D\hat{S}_z^2$ causes that the zero-field energy gap for the S = 3/2 spin system is $\Delta = 2D$, and not *D* as erroneously quoted. (ii) A possible role of the rhombic zero-field splitting parameter *E* is not discussed. (iii) The formula for the *x*-component of the magnetic susceptibility does not reproduce the experimental data in the present form. (iv) The anisotropy of the magnetogyric g-tensor is ignored in analysis of powder susceptibility data. (v) A possible misalignment of the *D*- and *g*-tensors is ignored. (vi) For a powder average a mean value of three Cartesian components is considered, which is clearly insufficient. (vii) The molecular field correction applied in the crystal *x*-direction is applied in an incorrect way. (viii) A rather high magnetic field (B = 0.5 T) is applied in acquiring the magnetic susceptibility data. (ix) A possible self-orientation of powder grains in higher magnetic fields is neither considered, nor discussed. (x) The magnetization data is missing and thus not analysed. (xi) The nature of the temperature-independent paramagnetism is not discussed; it is estimated empirically without any theoretical background. (xii) A possible effect of the residual field in the magnetometer is not investigated. The above drawbacks motivated us to study the magneto-chemical standard HgCo(NCS)$_4$ in a more detailed way.

The spin Hamiltonian for a mononuclear entity reads

$$\hat{H}_{kl} = D\hbar^{-2}(\hat{S}_z^2 - \bar{S}^2/3) + E\hbar^{-2}(\hat{S}_x^2 - \hat{S}_y^2) + \hat{H}_{kl}^{\mathrm{Z}} \qquad (1)$$

where the zero-field energy levels are determined by the axial zero-field splitting parameter *D*, and its orthorhombic counterpart *E*. Within this formalism the zero-field energy levels for the S = 3/2 spin system are represented by two Kramers doublets $|S, M_S\rangle$; their energy separation is $\Delta = 2(D^2 + 3E^2)^{1/2}$. In the present compound, however, the X-ray structure confirms a local D$_{2d}$ symmetry of the coordination polyhedron {CoN$_4$} and consequently the E-term can be safely omitted.

The Zeeman term for three Cartesian directions (a = x, y, z) is

$$\hat{H}_a^{\mathrm{Z}} = \mu_{\mathrm{B}} g_a B_a \hbar^{-1} \hat{S}_a \qquad (2)$$

and this can be applied for the single-crystal magnetization data. However, this is not true for the powder susceptibility (magnetization) so that an average $\bar{\chi} = (\chi_x + \chi_y + \chi_z)/3$ is incorrect when the magnetic anisotropy is substantial (when *D* is large).[8] The correct powder average requires an evaluation of the Zeeman term at a number of grids distributed uniformly over a sphere (one hemisphere) such us

$$\hat{H}_{kl}^{\mathrm{Z}} = \mu_{\mathrm{B}} B_m (g_x \sin\vartheta_k \cos\varphi_l \hat{S}_x + g_y \sin\vartheta_k \sin\varphi_l \hat{S}_y + g_z \cos\vartheta_k \hat{S}_z)\hbar^{-1} \qquad (3)$$

where (ϑ_k, φ_l) is a pair of polar angles; B_m – reference magnetic field. Then the diagonalization of the spin Hamiltonian yields a set of energy levels $\varepsilon_{m,i}(\vartheta_k, \varphi_l)$ which enter the partition function $Z_m(\vartheta_k, \varphi_l)$. Finally the magnetization $M_m(\vartheta_k, \varphi_l)$ and susceptibility $\chi_m(\vartheta_k, \varphi_l)$ are given by formulae of the statistical thermodynamics. To this end, the correct powder average requires integration that in the case of discrete points collapses to

---

[a] *Department of Chemistry, Faculty of Natural Sciences, University of Ss Cyril and Methodius, 917 01 Trnava, Slovakia; Email: roman.boca@ucm.sk*

[b] *National High Magnetic Field Laboratory, Florida State University, Tallahassee, Florida 32310, United States*

Electronic Supplementary Information (ESI) available: electronic spectra, details of *ab initio* calculations, EPR spectra, AC susceptibility data, three-level model for susceptibility. See DOI: 10.1039/x0xx00000x

$$\chi_{\mathrm{av}} = \frac{\sum_k \sum_l \chi(\vartheta_k, \varphi_l) \cdot \Delta_k(\cos\vartheta) \cdot \Delta_l(\varphi)}{\sum_k \sum_l \Delta_k(\cos\vartheta) \cdot \Delta_l(\varphi)} \quad (4)$$

and analogously for the magnetization. In order to secure a uniform distribution of the knots over a sphere a network of triangles can be generated (analogous to the EasySpin and SOPHE programs)[9] as follows: $\vartheta_k = (\pi/2)k/(K-1)$ and $\varphi_{kl} = 2\pi(l/k)$ with $k = 0, ..., K - 1$, and $l = 0, ..., k$; k refers to a number of knots along a meridian. The molecular field correction for the isotropic case, or in the z-direction only, is as simple as $\hat{H}_z^{\mathrm{mf}} = -(zj)\hbar^{-1}\langle S_z \rangle \hat{S}_z$ yielding

$$\chi_z^{\mathrm{cor}} = \mu_0 \frac{\partial M_z}{\partial B_z} = \frac{\chi_z}{1 - [(zj)/(k_{\mathrm{B}} C_0 g_z^2)] \cdot \chi_z} \quad (5)$$

An analogous formula cannot be applied for the x-direction, since the operator $\hat{H}_x^{\mathrm{mf}} = -(zj)\hbar^{-1}\langle S_x \rangle \hat{S}_x$ in the basis set of spin kets is non-diagonal; the eigenvalues need to be obtained through diagonalization of the corresponding interaction matrix. Then the Boltzmann average $\langle S_x \rangle$ is to be calculated in this new basis set. Consequently, a closed formula for the molecular-field correction does not exist so that the problem must be solved by an iteration procedure.

The compound HgCo(NCS)$_4$ (hereafter **1**) has been purchased from commercial sources,[$] ground to a fine powder, and encapsulated to a gelatine-made sample holder (m_s ~ 50 mg). The specimen was inserted into SQUID magnetometer (Quantum Design, MPMS-XL7).[‡] The applied field in the SQUID magnetometer is not measured directly. Thus when $B = 0$ is quoted, some residual field could be on (the Earth field plus some eddy field from the superconducting magnet). This effect can be investigated by mapping the linear regime of the magnetization of a paramagnetic sample when passing from the positive to negative fields: the intercept with the zero axis yields B_{res} that is identical for $T = 2.0$ and 4.6 K.

Uncorrected DC magnetic data for **1** are presented in Fig. 1. The magnetization data taken on the field-decreasing mode show that there exists a residual magnetic field $B_{\mathrm{res}} = 1.7$ mT for both temperatures $T = 2.0$ and 4.6 K, respectively. This means, that instead of the indicated field $B_0 = 0.1$ T the actual value is lower by 1.7 mT.

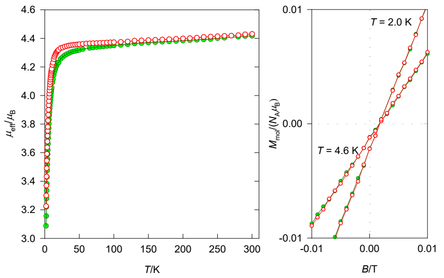

Figure 1. Uncorrected magnetic data for **1**. Left panel – temperature dependence of the effective magnetic moment; right panel – magnetization per formula unit. Four scans in the order: 1 – susceptibility for fresh sample (green), 2 – magnetization (green), 3 – repeated susceptibility (red, empty), 4 – repeated magnetization (red).

Using the field-corrected susceptibility data, the room-temperature value (300 K) of the effective magnetic moment adopts a value of $\mu_{\mathrm{eff}} = 4.38\ \mu_{\mathrm{B}}$ (Fig. 2). This is very close to data reported in literature.[1-7]

On cooling to moderate temperatures this value stays almost constant evidencing that the contributions to the overall temperature-independent magnetism of the sample (the underlying diamagnetism χ_{dia}, the temperature-independent paramagnetism χ_{TIP}, and diamagnetic signal of the sample holder χ_{sh}) nearly cancel. The underlying diamagnetism was estimated through a set of Pascal constants as $\chi_{\mathrm{dia}}(1) = -2.39 \times 10^{-9}$ m^3 mol^{-1} (SI units are used hereafter). An application of a frequently used approximation yields $\chi_{\mathrm{dia}}(2) = -5M_{\mathrm{r}} \times 10^{-9}$ m^3 mol^{-1} = -2.46×10^{-9} m^3 mol^{-1} (M_{r} given in SI units).

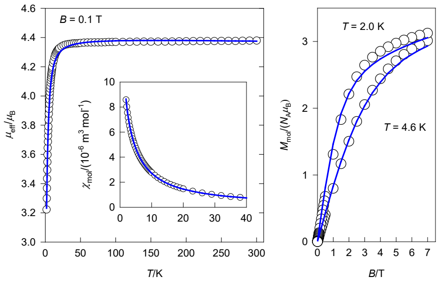

Figure 2. Magnetic data for fresh sample of **1** corrected for residual field, underlying diamagnetism and temperature-independent paramagnetism. Lines – fitted using spin Hamiltonian (see the text).

The TIP correction has been quoted as $\chi_{\mathrm{TIP}} = 5.40 \times 10^{-9}$ m^3 mol^{-1}.[7] The spin-Hamiltonian formalism for a tetracoordinate d^7 complex offers a closed formula [10]

$$\chi_{\mathrm{TIP}} = \frac{2}{3} N_{\mathrm{A}} \mu_0 \mu_{\mathrm{B}}^2 \left(2\frac{4\kappa_x^2}{\Delta_1(^4\mathrm{A}_2 \rightarrow {}^4\mathrm{T}_2)} + \frac{4\kappa_z^2}{\Delta_1(^4\mathrm{A}_2 \rightarrow {}^4\mathrm{T}_2)} \right) \quad (6)$$

where the orbital reduction factors and the electronic excitation energies occur. Making use the lowest excitation energy $10Dq = \Delta_1(^4\mathrm{A}_2 \rightarrow {}^4\mathrm{T}_2)$ = 5000 cm^{-1} we arrive at the result $\chi_{\mathrm{TIP}} = 5.24 \times 10^{-9}$ m^3 mol^{-1}.

The magnetic parameters have been calculated by means of the generalized crystal-field theory.[10] The experimental geometry of the D$_{2d}$ symmetry has been adopted with the strengths of the crystal-field poles $F_4 = 6750$ cm^{-1} ($10Dq = 5000$ cm^{-1}); notice $Dq(\mathrm{T_d}) = (4/9)Dq(\mathrm{O_h}) = (4/9)(1/6)F_4(R)$. The resulting set of the spin-Hamiltonian parameters is $g_z = 2.252$, $g_x = 2.294$, $D/hc = 3.65$ cm^{-1}, $E = 0$ and $\chi_{\mathrm{TIP}} = 5.30 \times 10^{-9}$ m^3 mol^{-1}. The zero-field energy gap given by the multiplet splitting is then $\Delta/hc = 6.37$ cm^{-1}.

The electronic spectrum of **1** shows two transitions in the NIR region followed by the intense transition in the Vis region (see SI). The lowest electronic excitation ^{4}A$_2$ ⟶ ^{4}T$_2$ is orbitally forbidden and probably refers so the band at 4500 cm^{-1}.[11] The band at 7000 cm^{-1} refers to the ^{4}A$_2$ ⟶ ^{4}T$_1$(F) transition and its energy is $\Delta_2 = 18Dq$. However, the configuration interaction between ^{4}T$_1$(F)...^{4}T$_1$(P) terms is effective and causes a reduction of the energy for this transition from expected 8100 to 7000 cm^{-1}. An estimate for the last allowed d-d transition ^{4}A$_2$ ⟶ ^{4}T$_1$(P) at 16 000 cm^{-1} is $\Delta_3 = 12Dq + 15B$; using Dq = 450 cm^{-1} the Racah parameter of Co(II) is estimated as $B = 707$ cm^{-1}. This value is lowered relative to the free-ion value (B_0 = 980 cm^{-1}) owing to the nephelauxetic effect. The assignment of the bands in the 16000 – 18000 cm^{-1} region is a bit intricate since the $^4T_1(P)$ mother term is split into {$^4A_2$, ^4E} daughter terms in the more realistic D_{2d} (or C_{2v}) group of symmetry. Moreover, the close-lying $^2E(G)$, $^2A_1(G)$, $^2T_1(G)$ and $^2T_2(G)$ terms might borrow the intensity from the spin-allowed transitions. The spin-orbit coupling is also in the play and it further modifies the term scheme.

The fitting procedure has been based upon the spin Hamiltonian (1) with the Zeeman term (3). The eigenvalues for the trial set of magnetic parameters and applied magnetic field were inserted into the partition function $Z(B,T)$; there points in vicinity of the experimental field value were used for a numerical determination of the first and second derivative from which the magnetization and susceptibility were evaluated by the apparatus of statistical thermodynamics.[8] No approximations were introduced in this stage so that the procedure is applicable for an arbitrary set of magnetic parameters and field values. An effective genetic algorithm has been applied in minimizing the error functional $F_1 = R(\chi)\times R(M)$ and/or $F_2 = w_1 R(\chi) + w_2 R(M)$ that account for the relative errors of susceptibility and magnetization. The resulting set of magnetic parameters is: g_z = 2.223, g_x = 2.292, D/hc = +3.86 cm^{-1}, χ_{TIM} = –1.0 × 10^{-9} m^3 mol^{-1}, $(zj/hc)g^2$ = –0.114 cm^{-1}. The discrepancy factor for susceptibility $R(\chi)$ = 0.0084 and for magnetization $R(M)$ = 0.034.

The set of magnetic parameters obtained by a simultaneous fitting of the susceptibility and magnetization data is close to the modelling by the generalized crystal-field theory. The self-consistency of the magnetic parameters can be checked by the spin-Hamiltonian formula $D = \lambda(g_z - g_x)/2$ where λ = –175 cm^{-1} is the spin-orbit splitting parameter for Co(II). Because $D > 0$, $g_z < g_x$ is expected.

Ab initio calculations for the fragment $[Co(NCS)_4]^{2-}$ predict the following spin Hamiltonian parameters: $\boldsymbol{g}$\{2.221 2.264, 2.264\}, D/hc = +3.41 cm^{-1} and E = 0.[#]

High-frequency and -field electron paramagnetic resonance (HFEPR)[‡] experiments on a $HgCo(NCS)_4$ powder gave strong and very broad spectra (Figs. 3, S4 and S5). Note that small ligands tend to have many degrees of freedom, which results in disorder at low temperatures, and affects the EPR linewidth. The spectra were identical for a loose powder, and a sample pressed into a pellet, which proved that no field-assisted aligning (torqueing) of the crystallites took place. The large line width results in a relatively low (by the HFEPR standards) precision in determining the spin Hamiltonian parameters.

Fig. 3 shows a typical HFEPR spectrum of a pellet, recorded at a frequency of 329 GHz (= ~11 cm^{-1}) that nearly corresponds to the zero-field gap between the two Kramers doublets. This allows for a quick estimate of the axial zfs parameter D as ~5.5 cm^{-1}. The simulations prove that the sign of D is positive. The final set of spin Hamiltonian parameters was obtained from the two-dimensional map of resonance fields *vs* frequency (Fig. 4): D = +5.39(2) cm^{-1}, g_z = 2.050(24), g_x = 2.161(7).

The AC susceptibility data for **1** are presented in Figs. 5 and 6. It can be seen that the system shows slow magnetic relaxation that strongly depends upon the external magnetic field. The nature of the slow magnetic relaxation is unknown so far; the Orbach relaxation mechanisms can be excluded owing to $D > 0$ and $E = 0$.

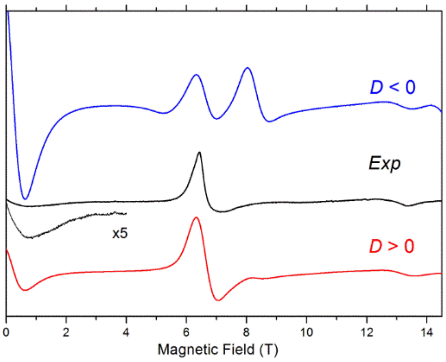

Figure 3. An HFEPR spectrum of $HgCo(NCS)_4$ at 10 K and 329 GHz (black trace). A near-zero field transition is clearly visible, which immediately yields D of ~5.5 cm^{-1} in the condition of E ~ 0 (which is confirmed by the single perpendicular intra-Kramers peak at 6.6 T.) Simulations use the following spin Hamiltonian parameters: $|D|$ = 5.39 cm^{-1}, g_{iso} = 2.18.

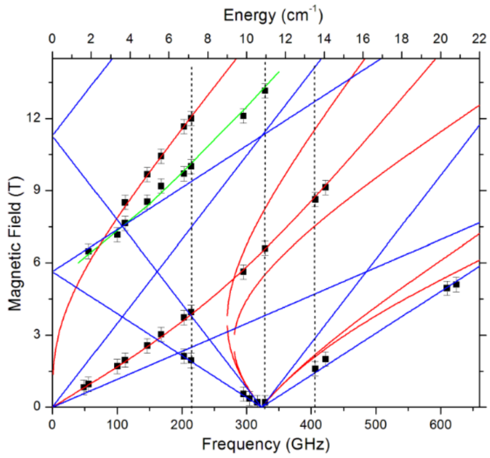

Figure 4. A two-dimensional field *vs* frequency (or energy) map of HFEPR resonances at 10 K. The squares are experimental points; the lines were drawn using spin Hamiltonian parameters as in the text. Red lines: turning points with magnetic field B_0 parallel to the x-axis of the zfs tensor; blue: B_0 || z; green: off-axis turning points. The error bars represent an average single-crystal line width (0.3 T) as obtained from powder spectra simulations. The dashed vertical lines represent the frequencies at which spectra shown in Figs. 3, S5, and S6 in increasing frequency order were recorded.

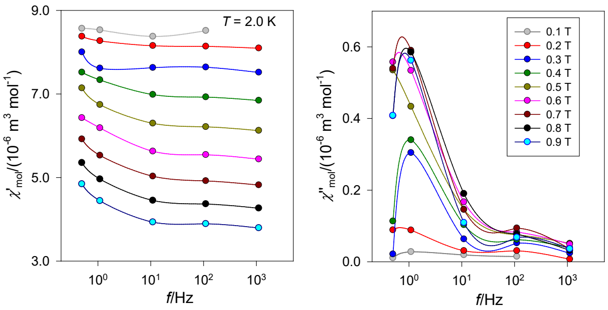

Figure 5. Frequency/field dependence of the AC susceptibility components of **1** at T = 2.0 K. Lines are guide for eyes.

Even more exciting is the existence of the low-frequency relaxation channel. For number of samples containing mononuclear complexes such a behaviour has been attributed to the presence of intermolecular contacts in the solid state. Such hypothesis is not supported by the crystal structure of **1**. There is a theoretical prediction based upon a three-level model that the second low-frequency channel can appear naturally (for modelling see SI).[19]

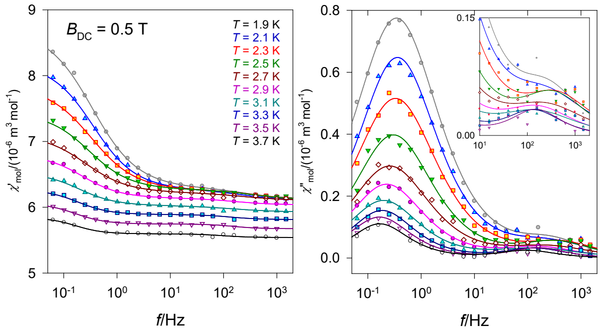

Figure 6. Dependence of the AC-susceptibility upon the frequency of the AC field and temperature at B_{DC} = 0.5 T for **1**. Lines – fitted with the two-set Debye model.

In conclusion, the {CoN$_4$} unit in **1** refers to a flattened tetrahedron (oblate disphenoid) of the D_{2d} symmetry with two N-Co-N angles >> 109 deg for which $D > 0$ holds true. In absence of E, the Orbach relaxation mechanism is excluded. This is in contrast to the frequent observations for elongated tetrahedrons (prolate disphenoids, two N-Co-N angles << 109 deg) where $D < 0$ is predicted in match with observations.[20,21]

Conflicts of interest

“There are no conflicts to declare”.

Notes and references

$ The X-ray structure of HgCo(NCS)$_4$ is available from the Inorganic Crystal Structure Database under the code ICSD 36062, available also from the CCDC 1607861. The tetragonal crystal system causes that the {CoN$_4$} unit is an elongated tetrahedron (prolate disphenoid) of D_{2d} symmetry.

‡ The measurements were conducted using the RSO mode of detection (amplitude A = 3 cm, frequency f = 1 Hz for susceptibility; A = 0.8 cm, f = 4 Hz for magnetization). The centring has been done at T = 5 K and B = 0.1 T. A fresh sample has been used free or any field-orientation. Data acquisition at B_0 = 0.1 T started at T = 1.9 K and finished at T = 300 K. Ample waiting period (400 s) has been applied after temperature stabilization before measurements. The recorded magnetic moment (m) of the specimen has been converted to the molar magnetic susceptibility $\chi_{\mathrm{mol}} = \mu_0 (m / B_0) M_{\mathrm{r}} / m_{\mathrm{s}}$ and consequently to the effective magnetic moment $\mu_{\mathrm{eff}} / \mu_{\mathrm{B}} = [(\chi_{\mathrm{mol}} T)3 / C_0)]^{1/2}$. The magnetization data were taken at T = 4.6 and 2.0 K, respectively in the field-decreasing mode (starting with B = 7 T) giving rise to molar magnetization $M_{\mathrm{mol}} = m \cdot M_{\mathrm{r}} / m_{\mathrm{s}}$. All data are presented in SI units, χ[SI] = 4π × 10^{-6} χ[cgs&emu]; the reduced Curie constant $C_0 = N_{\mathrm{A}} \mu_0 \mu_{\mathrm{B}}^2 / k_{\mathrm{B}}$ contains only the physical constants. The AC susceptibility measurements have been conducted with the same specimen; the amplitude of B_{AC} = 0.38 mT was applied. Note that the molar AC susceptibility is calculated by assuming a linear magnetic behaviour $\chi''_{\mathrm{AC}} = \mu_0 (m'' / B_{\mathrm{AC}})(M_{\mathrm{r}} / m_{\mathrm{s}})$.

The *ab initio* calculations were performed with ORCA 4.2.1 program for experimental geometry of the fragment [Co(NCS)$_4$]$^{2-}$.[13] Calculations were based on state average complete active space self-consistent field wave functions (SA-CASSCF) and N-electron valence second order perturbation theory (NEVPT2).[14,15] The minimal active space has been considered, comprised of seven electrons in five d-orbitals of the central atom. The state averaged approach was used, in which 10 quartet and 40 doublet states were equally weighted. Magnetic properties were modelled through quasi-degenerate perturbation theory in which an approximation to the Breit-Pauli form of the spin-orbit coupling operator (SOMF) was utilized.[16] The effective Hamiltonian theory was used for calculation of the ZFS parameters.[17] The relativistic effects were included in the calculations through the ZORA approximation together with the scalar relativistic contracted version of def2-TZVP basis functions for all elements.[18] RI approximation has been used with appropriate decontracted auxiliary basis set and the RIJCOSX approximation to exact exchange. Increased integration grids (Grid4 and GridX5) and tight SCF convergence criteria were set for the given calculation.

‡ High-frequency and -field electron paramagnetic resonance experiments were performed using a transmission spectrometer equipped with a 17 T superconducting magnet (Oxford Instruments) and a bolometer (QMC) as a detector. The operating frequencies were generated by Virginia Diodes Inc. (VDI) sources between 48 and 630 GHz. The sample was finely ground and pressed into a pellet with n-eicosane, or used ‘as is’. The measurements were done at T = 10 K. The data analysis was done using program SPIN.[12]

Author Contributions

The manuscript was written through contributions of all authors.

Grant agencies of Slovak Republic are acknowledged for the financial support (projects APVV 18-0016, 20-0032, and VEGA 1/0013/18). The HFEPR studies were supported by the NHMFL, which is funded by the National Science Foundation (Cooperative Agreement DMR 1157490 and 1644779) and the State of Florida. Dr. Andrew Ozarowski is acknowledged for his EPR fit and simulation software SPIN.

1 F. N. Figgis and R. S. Nyholm, *J. Chem. Soc.*, 1959, 338.
2 F. A. Cotton, D. M. L. Goodgame and M. Sacco. *J. Am. Chem. Soc.*, 1961, **83**, 4157.
3 H.-St. Rade, *J. Phys. Chem.*, 1973, **77**, 424.
4 J.-C. G. Bunzli, *Inorg. Chim. Acta.*, 1979, L413.
5 D. B. Brown, V. H. Crawford, J. W. Hall and W. E. Hatfield, *J. Phys. Chem.*, 1977, **81**, 1303.
6 C. J. O'Connor, E. Sinn, E. J. Cukauskas, and B. S. Deaver, *Inorg. Chim. Acta*, 1979, **32**, 29.
7 D. Nelson and L. W. ter Haar, *Inorg. Chem.*, 1993, ***32***, 182.
8 (a) R. Boča, *A Handbook of Magnetochemical Formulae*, Elsevier, Amsterdam, 2012; (b) R. Boča, *Theoretical Foundations of Molecular Magnetism*, Elsevier, Amsterdam, 1999.
9 S. Stoll and A. Schweiger, *J. Magn. Reson*., 2006, **178**, 42.
10 R. Boča, Magnetic Functions Beyond the Spin-Hamiltonian. *Struct. Bonding*, 2006, **117**, 1.
11 A. B. P. Lever, *Inorganic Electron Spectroscopy*, Elsevier, Amsterdam, 1968.
12 A. Ozarowski, *Program SPIN*. Private communication.
13 J. W. Jeffery and K. M. Rose, *Acta Cryst. B*, 1968, **24**, 653.
14 (a) F. Neese, The ORCA program system. Wiley Interdiscip. Rev.: Comput. Mol. Sci., 2012, **2**, 73; (b) F. Neese, ORCA-An Ab Initio, DFT and Semiempirical SCF MO Program Package, ver. 4.2.1; Max Planck Institute for Chemical Energy Conversion: Ruhr, Germany, 2018.
15 (a) C. Angeli, S. Borini, M. Cestari, M. and R. A. Cimiraglia, *J. Chem. Phys*., 2004, **121**, 4043; (b) C. Angeli, R. Cimiraglia, S. Evangelisti, T. Leininger, and J.-P. Malrieu, *J. Chem. Phys*. 2001, **114**, 10252; (c) C. Angeli, R. Cimiraglia and J.-P. Malrieu, *J. Chem. Phys.*, 2002, **117**, 9138.
16 F. Neese, *J. Chem. Phys.*, 2005, **122**, 34107.
17 (a) D. Ganyushin, and F. Neese, *J. Chem. Phys.*, 2006, **125**, 24103; (b) F. Neese, *J. Chem. Phys.* 2007, **127**, 164112.
18 (a) M. Filatov and D. Cremer, *Molecular Physics*, 2003, **101:14**, 2295. (b) F. Weigend, and R. Ahlrichs, *Phys. Chem. Chem. Phys.*, 2005, **7**, 3297; (c) F. Weigend, *Phys. Chem. Chem. Phys.*, 2006, **8**, 1057.
19 L.T.A. Ho and L. Chibotaru, *Phys. Rev. B.*, 2016, **94,** 104422.
20 Y. Rechkemmer, F. D. Breitgoff, M. van der Meer, M. Atanasov, M. Hakl, M. Orlita. P. Neugebauer, F. Neese, B. Sarkar and J. van Slageren, *Nature Comm*. 2016, **7**, 10467.
21 S. Vaidya, S. Tewary, S. K. Singh, S. K. Langley, K. S. Murray, Y. Lan,W. Wernsdorfer, G. Rajaraman and M. Shanmugam, *Inorg. Chem.* 2016, **55**, 9564.